EFFECTS OF FUEL ADDITIVES AND FUEL-OIL RATIO ON THE COMBUSTION CHARACTERISTICS AND PERFORMANCE OF A TWO-STROKE ENGINE

Mohamed N. Saeed
Mechanical Engineering Department, Faculty of Engineering,
Alexandria University, Alexandria, Egypt.

ABSTRACT

This paper investigates the effects of some operating parameters on the combustion characteristics, emissions, and fuel economy of a single-cylinder, two-stroke SI engine. The operating parameters include the engine speed, brake mean effective pressure, oil/fuel ratio, and the effect of immersing a tin-based catalyst in the fuel tank. Pressure histories were generated by an on-line data acquisition system. The histories were fed to a computer code for the thermodynamic analysis of the in-cylinder processes. Correlations were developed for the delivery ratio and brake specific fuel consumption in terms of the brake mean effective pressure. Although the fuel additive shortened the ignition delay and slightly increased the maximum heat flux, there was no significant reduction of exhaust emissions. The oil/fuel ratio affected neither the heat flux nor the emissions. When compared to the sinusoidal model of combustion, the exponential model predicts higher peak rates of heat release that occur near the end of the burning period.

Keywords: Two-Stroke, Fuel additive.

NOMENCLATURE

ATC	after top dead center
BMEP	brake mean effective pressure, kPa
BSFC	brake specific fuel consumption, kg/(kW.h)
BTC	before top dead center
DR	delivery ratio (defined in Appendix B)
E_{sc}	scavenging efficiency (defined in Appendix B)
E_{tr}	trapping efficiency (defined in Appendix B)
N	exponential index of combustion, nondimensional
O/F	oil/fuel ratio, by volume
P	pressure, kPa
P_b	brake mean effective pressure, kPa
S_p	mean piston speed, m/s
T_{ex}	exhaust temperature, °C
V	volume, m^3

Greek

θ	crank angle (measured from bottom center), degrees
ϕ	equivalence ratio

INTRODUCTION

The two-stroke engine is a strong competitor and a possible alternative to four-stroke engines because of its superior power-to-weight ratio, fewer components, and smaller size. However, two-stroke engines have been looked upon as a major challenge under the stringent emission regulations of 1994 and beyond. Fortunately, the recent advances in both scavenging technology and electronically controlled fuel injection have led to reducing specific fuel consumption as well as emission levels associated with these engines. Accordingly, the California Legislature in the 1990-91 State Budget directed the Department of Transportation (Caltrans) toward evaluating alternative propulsion systems and the possible implementation of two-stroke engines [1].

Among the numerous investigations conducted on two-stroke engines [2,3,4], the majority have been directed toward the improvement of scavenging and fuel economy [5-16]. Emission-control studies have come second on the priority list [17-27]. In addition, some works [28-30] were published on irregular combustion and cyclic variations while computer-modeling studies [29,31-37] were significantly fewer than models of four-stroke engines.

The recent advances in two-stroke engine design have required the use of leaner oil/fuel ratios in order to reduce spark-plug fouling, decelerate the formation of combustion chamber deposits, and lower visible smoke and hydrocarbon emissions. There is also a trend toward using tin-based catalysts (in the form of pellets immersed in the fuel tank) for the purposes of improving fuel economy, lowering emissions, and reducing friction. Because the indexed literature on these new trends is either very limited [19,21] or commercially oriented [38,39], the present paper is a systematic approach for investigating the effects of oil/fuel ratio and a tin-based fuel catalyst on the combustion characteristics and performance of a two-stroke SI engine.

EXPERIMENTAL APPARATUS AND PROCEDURES

The experiments were conducted on a single-cylinder, two-stroke SI engine (Appendix A). In order to measure the brake torque, the engine is coupled to a hydraulic dynamometer (TQ model TD 115). The flow of dynamometer water is controlled by a needle valve. The engine speed is measured by a pulse-counting system. An optical head mounted on the dynamometer chassis contains an infrared transmitter and receiver. A rotating disc with radial slots is situated between the optical source and sensor. The beam is interrupted as the engine rotates. The resulting pulses are electronically processed to provide a readout of engine speed. Temperatures of intake charge and exhaust gases are measured by a K-type chromel-alumel thermocouples. Average pressures at the intake and exhaust ports are measured by pressure gauges. Fuel consumption is measured by the constant-volume method through one of three pipettes of volumes 8, 16, and 32 milliliters. The rate of air flow is measured by a viscous flowmeter. The cylinder pressure is measured by a piezo-electric water-cooled pressure transducer (AVL model 8QP 500C). The crank-angle signal is generated by a TQ shaft encoder. Pressure histories are generated by an on-line data acquisition system. The histories are fed to a computer code for the thermodynamic analysis of the in-cylinder processes. A Richard Oliver multigas analyzer was used for determining the concentrations of exhaust emissions. The system has a flame ionization detector (FID) for total hydrocarbons (THC), a nondispersive infrared (NDIR) module for CO and CO_2, a paramagnetic sensor for O_2, and a chemiluminescent analyzer for NOX. The sampling tube is fitted to the tailpipe 280 mm away from the exhaust port in order to allow sufficient mixing of exhaust gases. Figure (1) shows a schematic of the engine and its instrumentation.

When performance tests were run on the engine, it was found that a wide range of torques was possible only when the engine was operated at a constant speed of 3550 ± 50 RPM. It was also found that the constant torque of 4 N.m was the most suitable one for a wide range of speeds between 2600 and 4400 RPM. When other settings were attempted, engine operation was unstable, and steady-state performance could not be achieved. Three mixtures of fuel/lubricating oil were tested. The oil/fuel ratios were 2:100, 4:100, and 6:100. The sets of experiments were run with and without the fuel catalyst. Before switching to a new fuel, the engine was allowed to run for sufficient time to consume the fuel remaining from the past set of experiments.

RESULTS AND DISCUSSIONS

1. Performance. The effects of various parameters on the delivery ratio are shown in Figure (2). The figure (Fig. 2.a, b) suggests a linear correlation between the brake mean effective pressure (or torque) and the delivery ratio in the form:

$$DR = K_1 \, (P_b / 100) + K_2 \qquad (1)$$

where DR is the delivery ratio and P_b is the brake mean effective pressure, kPa. The constants K_1 and K_2 depend, in principle, on the oil/fuel ratio and whether the fuel contains catalyst or is catalyst-free.

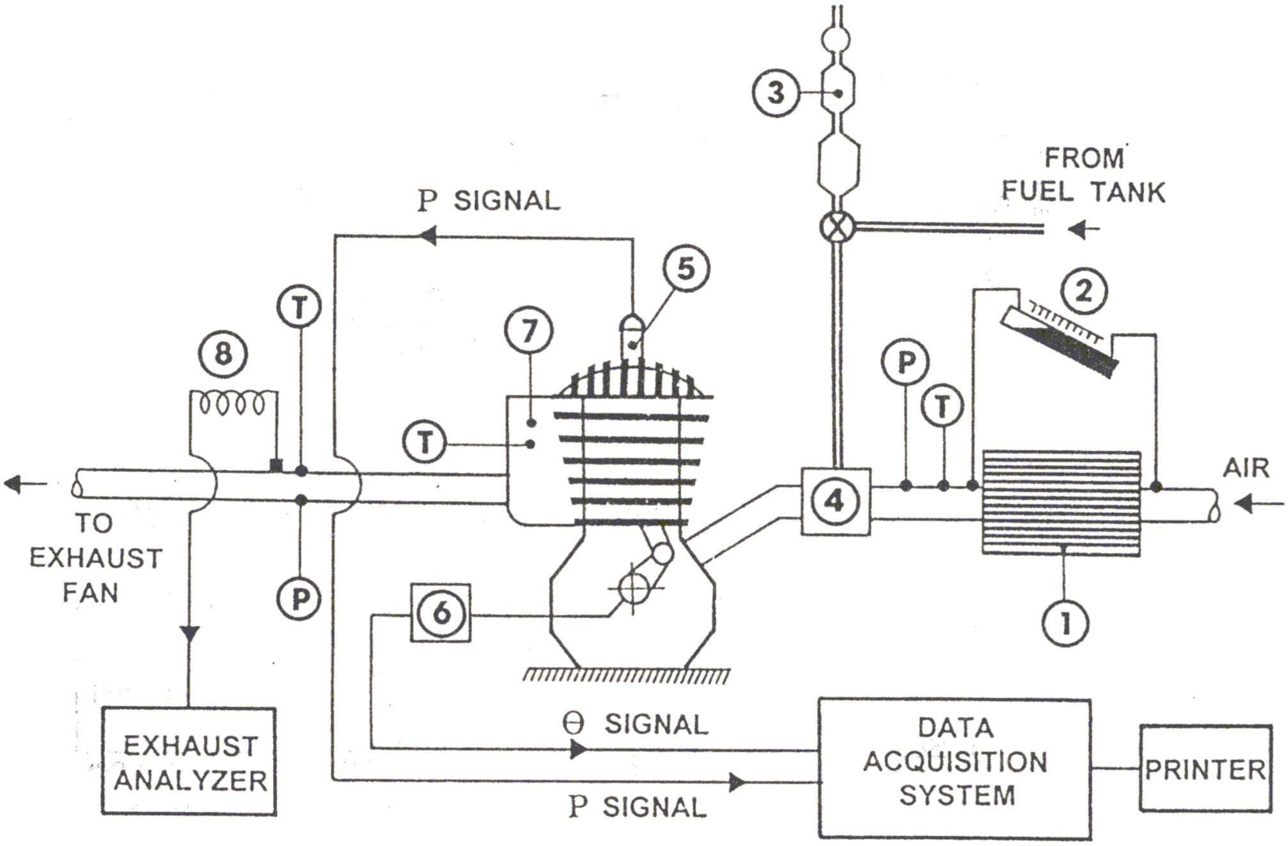

1.	Laminar Flowmeter	5.	Pressure Transducer
2.	Manometer	6.	Shaft Encoder
3.	Burette	7.	Exhaust Box
4.	Carburettor	8.	Sampling Tube

Figure 1. Schematic of engine and instrumentation.

The delivery ratio has a range of values between 0.25 at low BMEP and 0.65 at high BMEP. On the other hand, the effect of engine speed on the delivery ratio was not a straight-forward relationship (Figure (2.c, d)). The figure shows a slight increase in the delivery ratio as the speed is increased up to 3000 RPM. The ratio then decreases with higher speeds up to 3300 RPM, and increases again as the speed is further increased to 3800 RPM. Higher speeds up to 4400 RPM did not show significant changes in the delivery ratio. This trend agrees, in general, with the literature [7,18,26,27]. The use of the tin-based fuel catalyst did not have a significant effect on the delivery ratio, and neither did the variation of the oil/ fuel ratio (O/F). Therefore, Eq.(1) may correlate all fuels under investigation at the constant speed of 3550 RPM. As a result of using 82 data points for this correlation (Fig. 3), the correlation coefficient is 0.7809 whereas the values of K_1 and K_2 are 0.1038 kPa^{-1} and 0.2523, respectively.

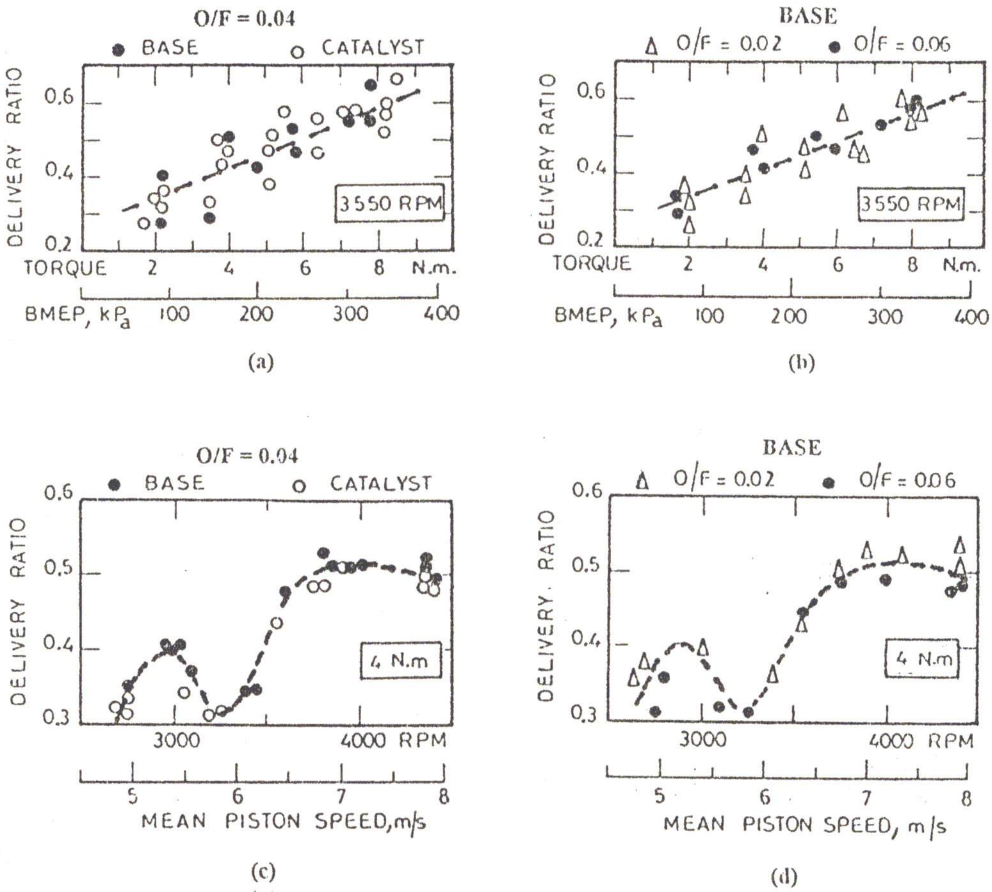

Figure 2. Parameters affecting delivery ratio.
a- BMEP and fuel type b- BMEP and O/F ratio
c- Speed and fuel type d- Speed and O/F ratio

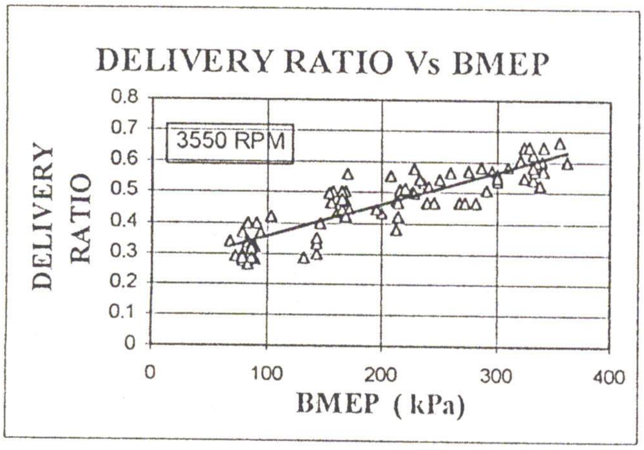

Figure 3. Delivery-ratio correlation.

The equivalence ratio (ϕ) is plotted in Figure (4) vs the torque demand (Fig. 4.a,b) and the speed demand (Figure (4.c, d)). The figure shows that the required equivalence ratio increases from a near-stoichiometric value at low torques to a rich value of 1.5 as the torque increases to 4 N.m (BMEP= 166 kPa). The equivalence ratio remains unchanged at greater torques (Figure (4.a, b)). The effect of speed, however, shows another trend (Figure (4.c, d)) where two speed zones are clearly distinguished with their equivalence-ratio requirements. For speeds lower than 3400 RPM, a near-stoichiometric mixture is required while very rich mixtures are necessary for stable operation at speeds higher than 3500 RPM. Similar trends were reported by Laimbock [24] and Poola et al. [27]. Again, neither the fuel catalyst nor the oil/fuel ratio has a considerable effect on the equivalence ratio.

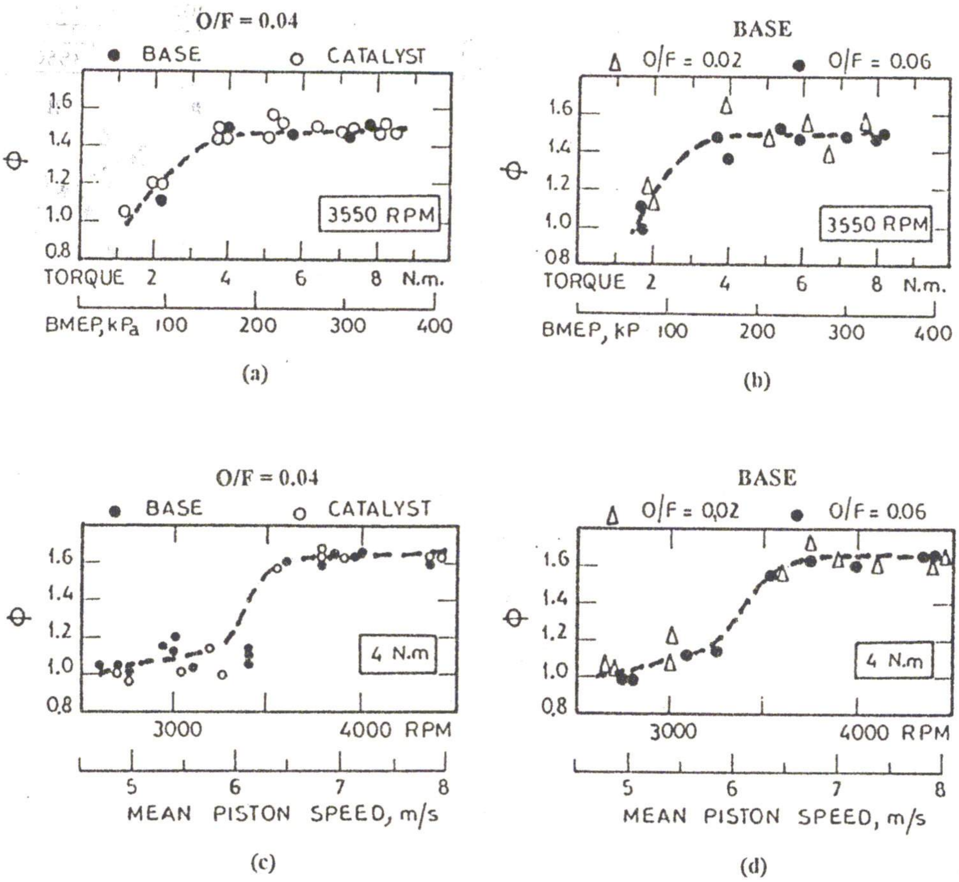

Figure 4. Parameters affecting equivalence ratio

a- BMEP and fuel ratio b- BMEP and O/F ratio

c- Speed and fuel type d- Speed and O/F ratio

The fuel economy, as represented by the brake specific fuel consumption (BSFC), is shown in Figure (5). The figure shows a linear correlation between the BMEP (or torque) and the BSFC (Figure (5.a,b)) in which fuel economy improves with greater torques. The correlation is given by:

$$BSFC = K_3 \left(P_b / 100 \right) + K_4 \qquad (2)$$

where BSFC has the units of kg/(kW.h).

It has been found that neither the oil/fuel ratio nor the fuel catalyst has a consistently pronounced effect on fuel economy. Therefore, Eq.(2) may correlate all fuels investigated at the constant speed of 3550 RPM (Figure (6)). The correlation coefficient is 0.8354 whereas K_3 and K_4 have the values of -0.2618 kg/(kW.h) per kPa and 1.5210 kg/(kW.h), respectively. On the other hand, the BSFC shows a sudden increase as the engine speed is increased beyond 3500 RPM (Figure (5.c,d)). This latter trend looks similar to that pronounced by the equivalence ratio (Figure (4.c,d)).

The exhaust temperature at exhaust port ranges between 425 and 500°C for torques lower than 5 N.m (BMEP ≈ 200 kPa), and between 600 and 650°C for torques higher than 5 N.m (Figure (7.a)). On the other hand, it is noticed that the exhaust temperature, as measured in the tailpipe (250 mm downstream), increases linearly with the BMEP as follows:

$$T_{ex} = K_5 \, P_b + K_6 \qquad (3.a)$$

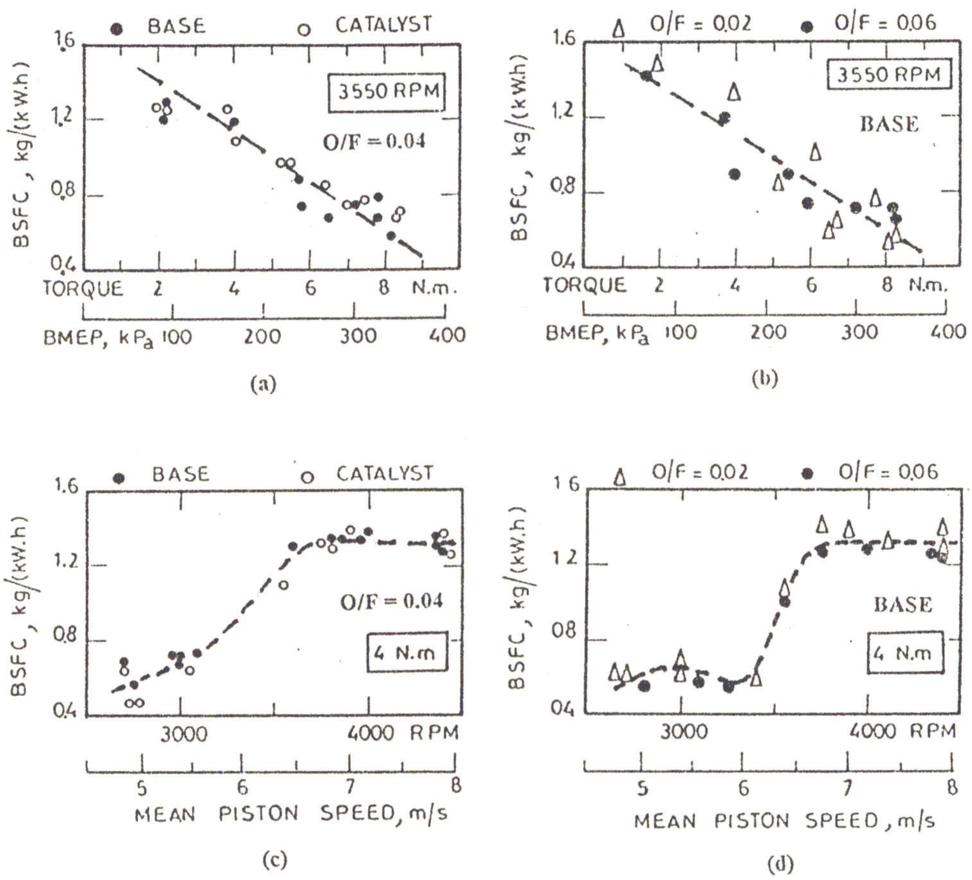

Figure 5. Parameters affecting BSFC

a- BMEP and fuel ratio b- BMEP and O/F ratio

c- Speed and fuel type d- Speed and O/F ratio

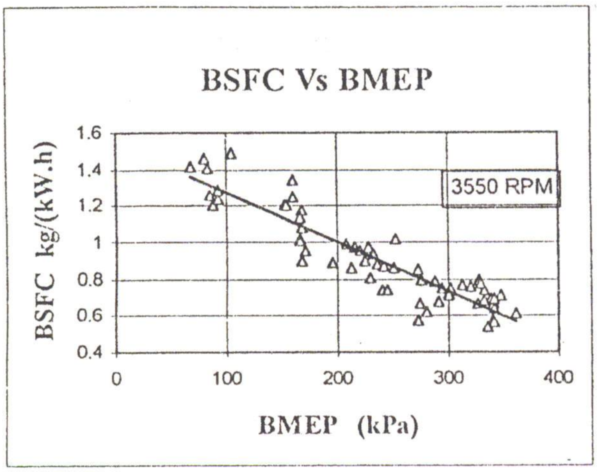

Figure 6. BSFC correlation.

where T_{ex} is the exhaust temperature (°C), measured in the tailpipe (250 mm downstream of exhaust port). The effect of engine speed on the exhaust temperature is shown in Figure (7.b) where the port temperature ranges between 550 and 620°C for speeds lower than 3300 RPM. However, a sudden drop in the port temperature is observed for speeds higher than 3300 RPM. In the meantime, tailpipe temperature increases linearly with mean piston speed as follows:

$$T_{ex} = K_7\ S_p + K_8 \qquad (3.b)$$

where S_p is the mean piston speed (m/s).

Figure (7) also shows no influence whether the oil/fuel ratio is varied or when the fuel catalyst is used. Therefore, Eq.(3.a) may correlate all fuels investigated at the constant speed of 3550 RPM (Figure (8.a)), while Eq.(3.b) may correlate all fuels investigated (Figure (8.b)) at the constant torque of 4 N.m (BMEP= 166 kPa). The constants are:

K_5 = 0.718 °C/kPa K_6 = 111.84 °C
K_7 = 21.69 °C/(m/s) K_8 = 125.94 °C

The correlation coefficients for Eqs.(3.a) and (3.b) are 0.9420 and 0.8554, respectively.

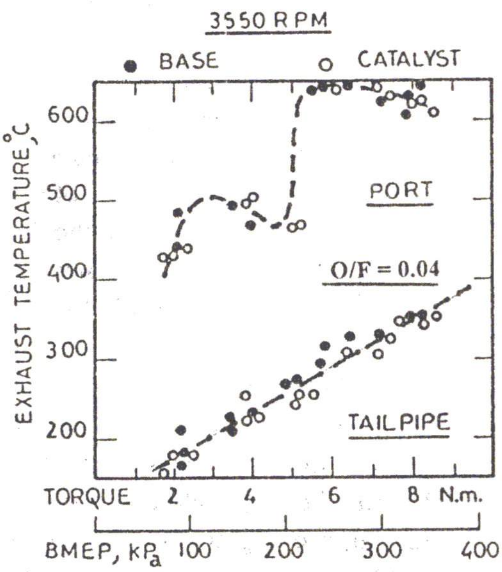

(a)

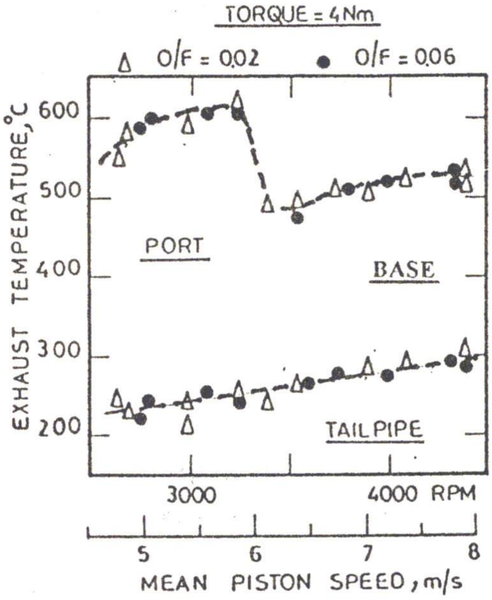

(b)

Figure 7. Parameters affecting exhaust temperature.
a- BMEP and fuel type b- Speed and O/F ratio

2. Emissions. Because the engine was run on rich mixtures at all times, there was no significant variations in the amounts of emitted NOX, HC, and CO. The NOX concentrations were in the range of 20-60 PPM. These values are in reasonable agreement with the literature [17] where concentrations in the order of 100 ppm were reported for air/fuel ratios in the rang of 10:1 - 12:1. The HC emissions exceeded the maximum value of 5000 PPM that can be measured by the exhaust analyzer. Some references [17,18] reported HC concentrations about 6000 PPM for air/fuel ratios between 10:1 - 14:1, while others [19,26,27,30] reported HC emissions over a very wide range between 2000 and 80000 PPM. Moreover, it was found [19] that the oil/fuel ratio has no significant effect on hydrocarbon emissions. The CO emissions were almost constant at 9.6 %. This number agrees with the value of 10% that was reported by Yamagishi et al.[17] for the air/fuel ratio of 10:1. As for the CO_2 emissions, the results Figure (9) show that speeds lower than 3400 RPM are associated with high emissions as compared to emissions at speeds above 3500 RPM. On the other hand, the O_2 emissions are much lower at low speeds than at high speeds. The present values of oxygen concentrations are comparable to those reported by Tsuchiya and Hirano [18] as 6-8 %. It is obvious that Figure 9 is closely related to Figures (4) and (7) which show a slightly rich combustion at high temperature when the engine speed is below 3400 RPM. The oxidation rate is high enough to produce the high rate of CO_2 emissions. On the other hand, combustion becomes excessively rich at high speeds. The resulting drop in temperature impedes the oxidation rate and causes a reduction in CO_2 emissions. As for the effect of the tin-based fuel catalyst on emissions, the present results show no significant improvement in emission levels.

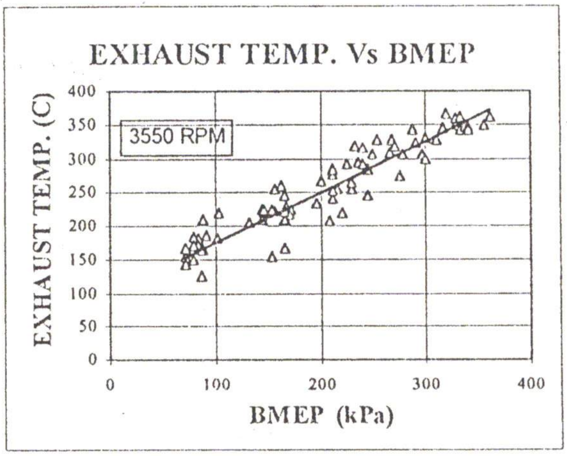

(a)

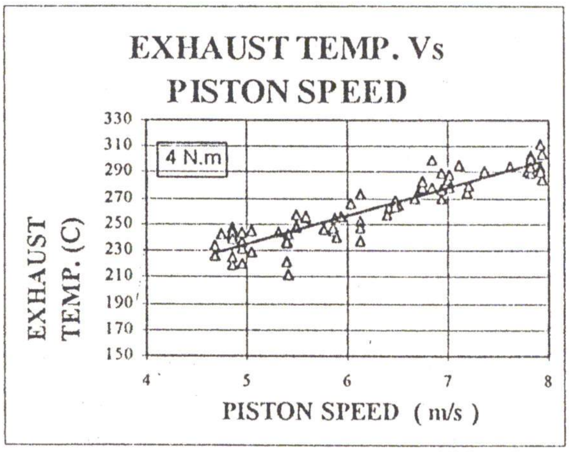

(b)

(b)

Figure 8. Exhaust temperature correlations
a- Speed = 3550 RPM b- Torque = 4 N.m.

3. Heat Release. Based on a review of literature [29-37], the heat-release analysis was performed through a single-zone model. The fuel-air charge was assumed to follow the complete-mixing model in which the entrapped fresh charge and residual gases behave as a homogeneous mixture [40,41]. The gas processes during compression and expansion followed the ideal-gas assumption. The specific heats were considered as temperature dependent [40-44]. The exhaust composition in the model was determined from the stoichiometry of the combustible mixture. The effect of NOX emissions on exhaust composition was assumed negligible. The rates of heat release were calculated by three models: linear, exponential, and sinusoidal [41]. The heat flux through engine walls was calculated from the first law of thermodynamics on the basis of the P-V data and heat-release calculations.

Figure (10) shows the effect of speed on both the rate of pressure change and the heat flux through cylinder walls. The figure shows similar patterns of $dP/d\theta$ with peak and valley values in the order of 30 and -20 kPa/deg, respectively. As for the heat flux, it is obvious that the heat transfer coefficients increase as the speed is increased, which results in more heat flux. In addition, both the delivery ratio DR and the equivalence ratio ϕ increase with increasing the engine speed, as shown in Figures (2) and (4), respectively. This leads to resulting increases in each of the trapping efficiency E_{tr} (Appendix B), the mass of fuel burned per kilogram of cylinder contents and, of course, the associated increase in heat flux. The figure also shows that a positive heat flux takes place during the expansion stoke for $210° < \theta < 240°$ due to the cooling effect of fast expansion and the resulting reversed heat transfer from cylinder walls to the expanding gases. This interesting phenomenon which has previously been reported in the literature [45, 46] can be explained in the light of both the first law of thermodynamics and the boundary layer theory. During the stage of fast expansion, the gas temperature in the immediate vicinity of the cylinder wall falls below the wall temperature although the bulk temperature of the gas at the outer edge of the boundary layer is higher than the wall temperature. The result is a positive (inward) heat flux that persists until the rate of work done decreases. As the piston approaches the bottom center, the heat flux becomes negative (outward).

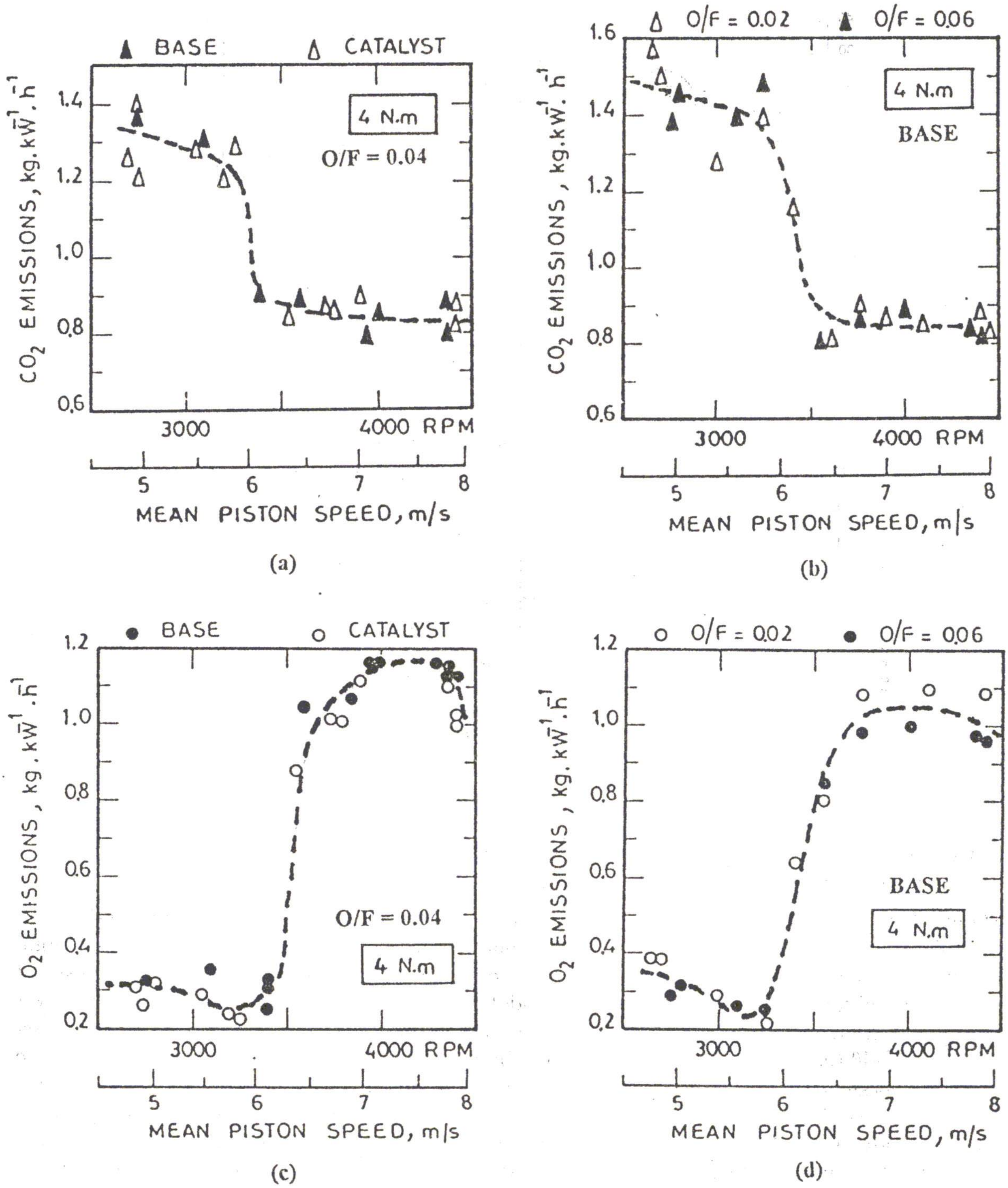

Figure 9. Parameters affecting exhaust emissions
a- CO_2; speed and fuel type b- CO_2; speed and O/F ratio
c- O_2; speed and fuel type d- O_2; speed and O/F ratio.

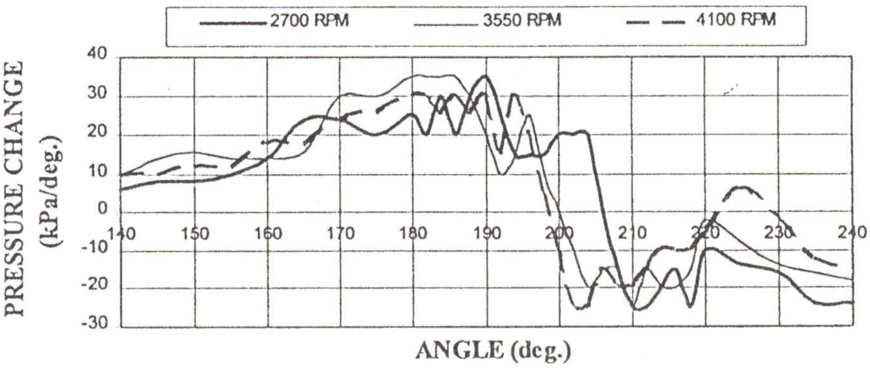

(a)

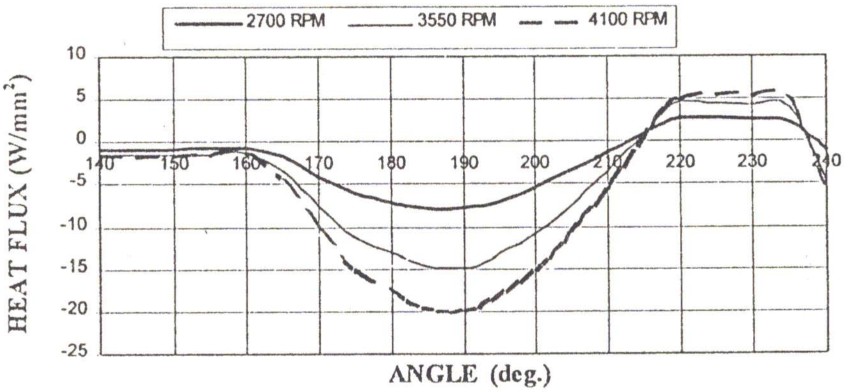

(b)

Figure 10. Effects of speed on combustion phenomena
a- Rate of pressure change b- Heat flux.

Figure (11) shows that the oil/fuel ratio does not have a pronounced effect on either the rate of pressure change or the heat flux.

Figure (12) shows that adding a tin-based catalyst to the fuel shortens the ignition lag of the fuel such that the zero value of $dP/d\theta$ (corresponding to peak pressure) moves by approximately 10° towards the top center. On the other hand, the maximum heat flux shows a slight increase from 21 to 23 W/mm^2.

Figure (13) shows that the heat flux increases with the increase in the trapping efficiency. The figure also shows that the maximum heat flux occurs at 5° ATC for the trapping efficiency of 0.2, then keeps shifting away from the top center towards 10° ATC for the ideal trapping efficiency of 1.0.

The comparison between the different models of heat release is shown in Figure (14). The exponential model provides the highest maximum rate of heat release followed by the sinusoidal model. The linear model produces both the lowest rate of maximum heat release and the least maximum heat flux. It is also shown that the maximum rate of heat release occurs very late (218°) in the case of the exponential model, and closer to the top center (192°) in the case of the sinusoidal model. The linear model shows a constant value of heat release rate throughout the combustion period. However, the value of heat flux decreases in the linear model, as combustion progresses, due to the increase in the area of heat transfer during expansion.

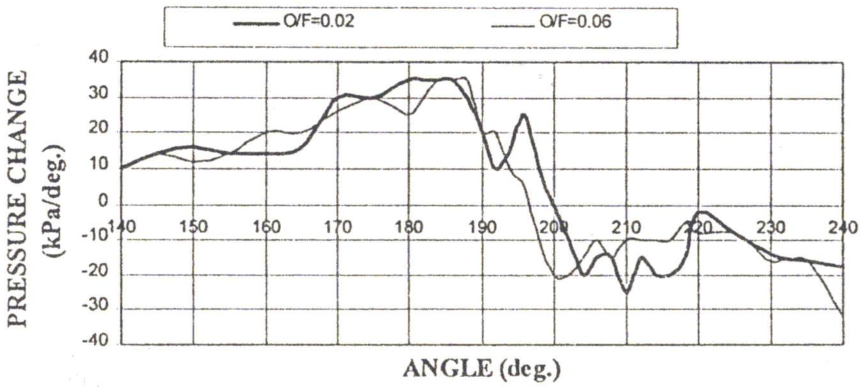

(a)

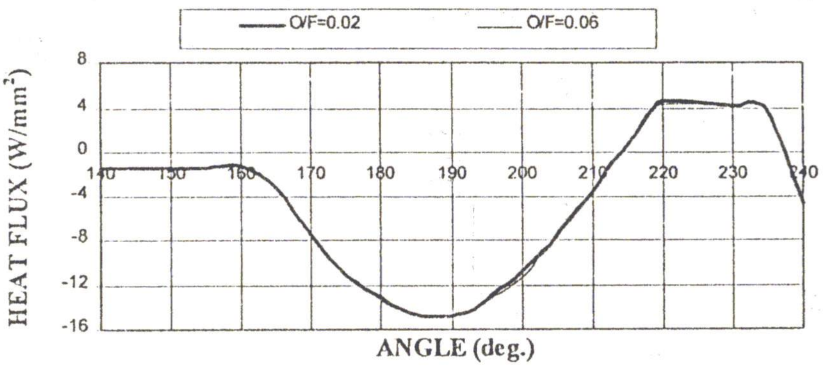

(b)

Figure 11. Effects of oil-fuel ratio on combustion phenomena
a- Rate of pressure change b- Heat flux.

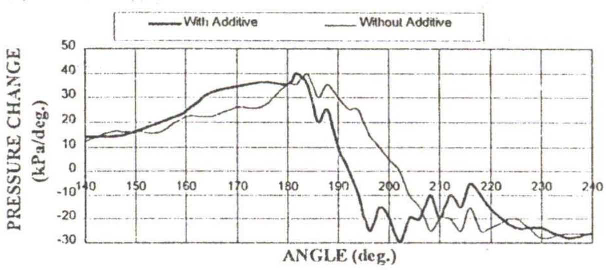

(a)

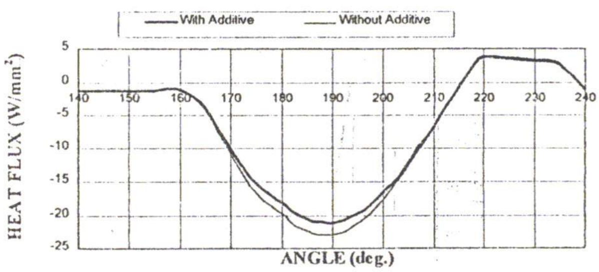

(b)

Figure 12. Effects of fuel additive on combustion phenomena
a- Rate of pressure change b- Heat flux.

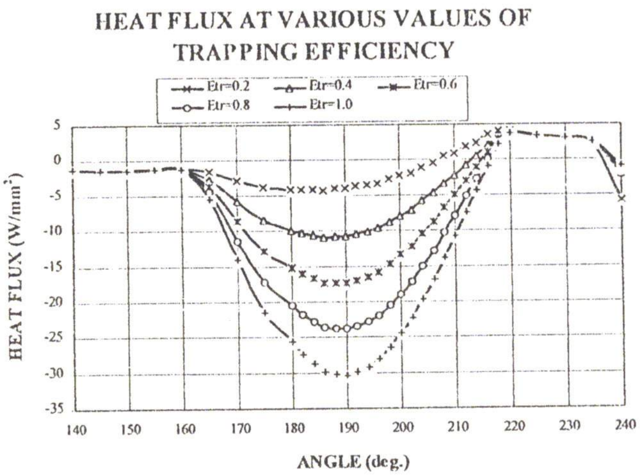

Figure 13. Effect of trapping efficiency on heat flux.

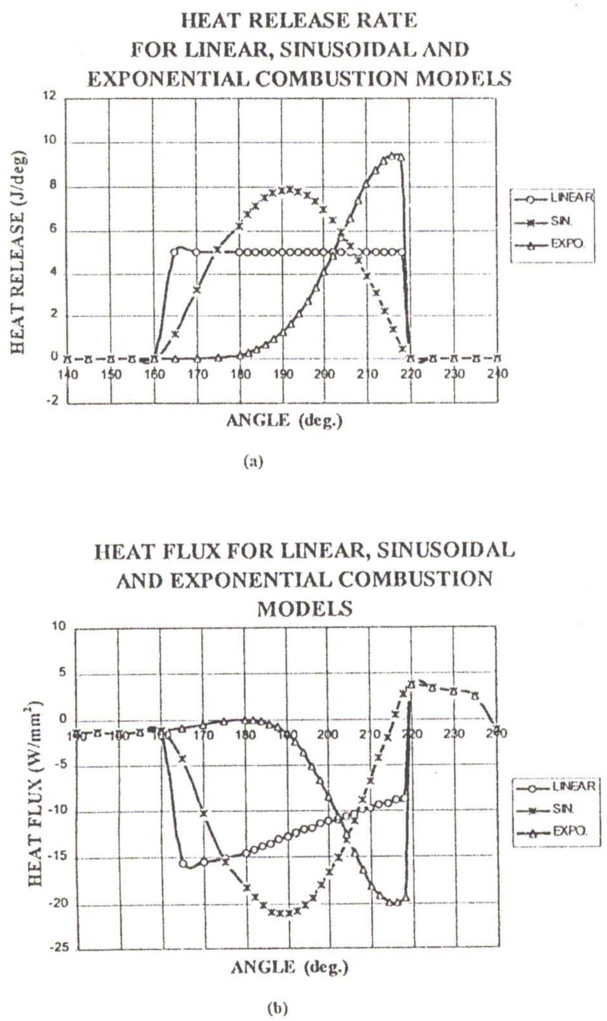

Figure 14. Comparison of heat-release models
a- Rate of heat release b- Heat flux.

Figure (15) shows the heat release and the heat flux for the exponential indices 4, 5, and 6 in the exponential model of combustion. The figure shows that during the early stages of combustion, both heat release and heat flux increase with decreasing the index N. However, as the combustion proceeds, the opposite effect occur at approximately 25° ATC, where a greater exponent results in a higher rate of heat release and greater heat flux.

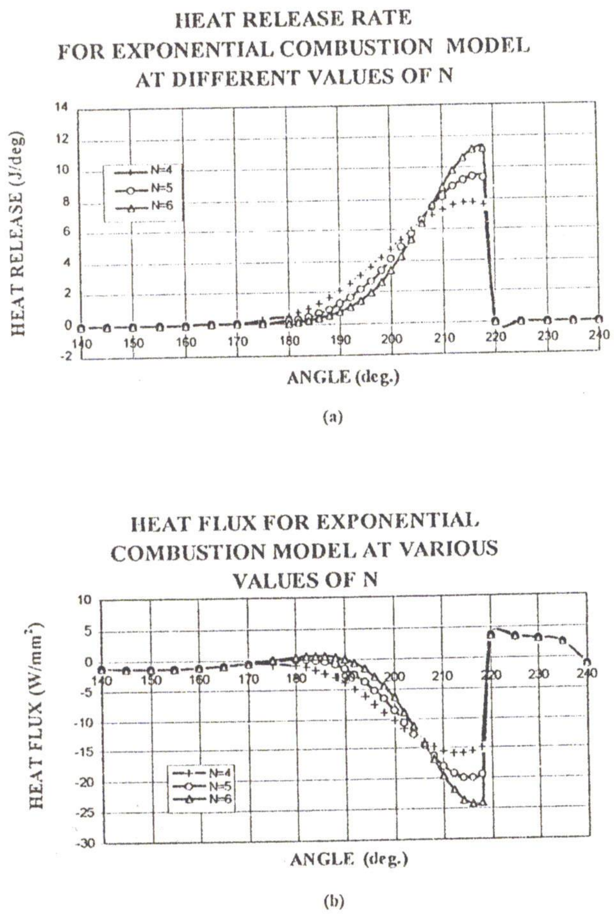

Figure 15. Effects of exponent on combustion phenomena
a- Rate of heat release b- Heat flux.

CONCLUDING REMARKS

Experiments have been conducted on a single-cylinder, two-stroke SI engine. Performance parameters and exhaust emissions have been measured. The histories of cylinder pressure have been used for performing the heat-release analysis.

The following concluding remarks are drawn:

1. Correlations have been developed for the delivery ratio and brake specific fuel consumption in terms of the brake mean effective pressure. The results show improvements in both delivery ratio and fuel economy with higher torque demands.
2. The exhaust temperature, as measured in the tailpipe, has been correlated in terms of the brake mean effective pressure and mean piston speed.
3. The addition of a tin-based catalyst to the fuel has not produced a significant reduction of exhaust emissions. However, the additive has shortened the ignition lag and has slightly increased the maximum heat flux.
4. The emissions of CO, CO_2, and NOX have not been affected by the oil/fuel ratio, and neither have the histories of cylinder pressure and heat flux.
5. The increase in trapping efficiency delays the occurrence of maximum heat flux.
6. The exponential model of combustion predicts relatively high peak rates of heat release that occur near the end of the burning period. The sinusoidal model predicts slightly lower peak rates that occur in the middle of burning period.
7. Increasing the index N in the exponential model of combustion decreases both the rate of heat release and the heat flux during the early stages of combustion, and increases them during the later stages. It has been found that the inflection point for this behaviour occurs at approximately 25° ATC.

REFERENCES

[1] F.A.Wyczalek, " Two-Stroke Engine Technology in the 1990's," *SAE Tech Paper*, No. 910663, SAE Intl Congress and Expo, Detroit, Michigan, Feb 25- March 1, 1991.

[2] G.P.Blair, R.R.Booy, and B.L.Sheaffer (Editors), *Technology Pertaining to Two-Stroke Cycle Engines*, PT-26, Society of Automotive Engineers, Warrendale Pennsylvania, ISBN 0-89883-114-8, 1982.

[3] G.P.Blair, G.Lassanske, and B.L.Sheaffer (Editors), *Advances in Two-Stroke Cycle Engine Technology*, PT-33, Society of Automotive Engineers, Warrendale Pennsylvania, ISBN 0-89883-120-2, 1989.

[4] E.G. Groff and B.L. Sheaffer (Editors), *Two-Stroke Engine Diagnostics and Design*," SP-901, Society of Automotive Engineers, Warrendale, Pennsylvania, ISBN 1-56091-218-9, 1992.

[5] P.H.Schweitzer and H.Grunder, "Hybrid Engines," *SAE Tech Paper*, No. 549 A , 1963.

[6] E.W. Huber, "Measuring the Trapping Efficiency of Internal Combustion Engines through Continuous Exhaust Gas Analysis ," *SAE Tech Paper*, No. 710144, Auto- motive Engineering Congress & Expo, Detroit, Michigan, January, 1971.

[7] G.P. Blair and R.G. Kenny, "Further Developments in Scavenging Analysis for Two-Cycle Engines," *SAE Tech Paper*, No. 800038 , SAE Intl Congress & Expo, Detroit, Michigan, February, 1980.

[8] D.S.Sanborn, G.P.Blair, R.G.Kenny, and A.H.Kingsburry, "Experimental Assess-ment of Scavenging Efficiency in Two-Stroke Cycle Engines," *SAE Tech Paper*, No. 800975, SAE Intl Off-Highway Mtg & Expo, Milwaukee, Wisconsin, September, 1980.

[9] N. Hata, T. Fujita and N. Matsuo, " Modification of Two-Stroke Engine Intake System for Improvements of Fuel Consumption and Performance through Yamaha Energy Induction System (YEIS)," *SAE Tech Paper*, No. 810923, Intl Off-Highway Mtg & Expo, Milwaukee, Wisconsin, September, 1981.

[10] G.P. Blair, B.W. Hill, A.J. Miller, and S.P.Nickell, "Reduction of Fuel Consum-ption of a Spark-Ignition Two-Stroke Cycle Engines," *SAE Tech Paper*, No. 830093, SAE Intl Congress & Expo, Detroit, Michigan, 1983.

[11] B.W. Hill and G.P. Blair, "Further Tests on Reducing Fuel Consumption with a Carburetted Two-Stroke Cycle Engine," *SAE Tech Paper*, No. 831303, SAE Intl Off-Highway Mtg & Expo, Milwaukee, Wisconsin, September, 1983.

[12] K. Nomura, S. Hirano, and Y. Motoyama, "Improvement of Fuel Consumption with Variable Exhaust Port Timing in a Two-

Stroke Gasoline Engine," *SAE Tech Paper*, No. 850183, SAE Intl Congress & Expo, Detroit, Michigan, 1985.

[13] J.G. Smyth, R.G. Kenny and G.P. Blair, "Motored and Steady Flow Boundary Conditions Applied to the Prediction of Scavenging Flow in a Loop-Scavenged, Two-Stroke Cycle Engine," *SAE Tech Paper*, No. 900800, SAE Intl Congress & Expo, Detroit, Michigan, Feb 26 - March 2, 1990.

[14] G.P. Blair, "An Alternative Method for the Prediction of Unsteady Gas Flow through the Internal Combustion Engine," *SAE Tech Paper*, No. 911850, SAE Intl Off-Highway Mtg & Expo, Milwaukee, Wisconsin, September 9-12, 1991.

[15] B.J. Tobis, R. Meyer, J. Yang, D.D. Brehob, and R.W. Anderson, "Scavenging of a Firing Two-Stroke Spark-Ignition Engine," *SAE Tech Paper*, No. 940393, SAE Intl Congress & Expo, Detroit, Michigan, Feb 28- March 3, 1994.

[16] R. Fleck and D. Thornhill, "Single Cycle Scavenge Testing a Multi-Cylinder, Externally-Scavenged, Two-Stroke Engine with a Log Intake Manifold," *SAE Tech Paper*, No. 941684, SAE Intl Off-Highway & Powerplant Congress & Expo, Milwaukee, Wisconsin, September 12-14, 1994.

[17] G. Yamagishi, T. Sato and H. Iwasa, "A Study of Two-Stroke Cycle Fuel Injection Engines for Exhaust Gas Purification," *SAE Tech Paper*, No. 720195, SAE Auto Engrg Congress & Expo, Detroit, Michigan, 1972.

[18] K. Tsuchiya and S. Hirano, "Characteristics of 2-Stroke Motorcycle Exhaust HC Emission and Effects of Air-Fuel Ratio and Ignition Timing," *SAE Tech Paper*, No. 750908, SAE Auto Engrg and Manufacturing Mtg, Detroit, Michigan, 1975.

[19] K. Sugiura and M. Kagaya, "A Study of Visible Smoke Reduction from a Small Two-Stroke Engine Using Various Lubricants," *SAE Tech Paper*, No. 770623, SAE Fuels and Lubricants Mtg, Tulsa, Oklahoma, 1977.

[20] C.G.A. Eberan-Eberhorst and H. Martin, "Performance Test Method for Two-Stroke Cycle Engine Lubricants Including Lean Fuel_Oil Ratio Conditions," *SAE Tech Paper*, No. 790078, SAE Intl Congress & Expo, Detroit, Michigan, 1979.

[21] C.R. McCaffree and R.M. Jacobsen, "Future Two-Cycle Engine Oil Development -A New Challenge," *SAE Tech Paper*, No. 790079, SAE Intl Off-Highway Vehicle Mtg & Expo, Milwaukee, Wisconsin, September, 1979.

[22] K. Tsuchiya, S. Hirano, M.Okamura and T.Gotoh, "Emission Control of Two-Stroke Motorcycle Engines by the Butterfly Exhaust Valve ," *SAE Tech Paper*, No. 800973, SAE Intl Off-Highway Mtg & Expo, Milwaukee, Wisconsin, 1980.

[23] Anonymous, *Test Procedure for the Measurement of Exhaust Emissions from Small Utility Engines- SAE Recommended Practice J* 1088, JUN 1983," Society of Automotive Engineers, Warrendale, Pennsylvania, June, 1983.

[24] F.J. Laimbock, "The Potential of Small Loop-Scavenged, Spark-Ignition, Single-Cylinder, Two-Stroke Engines," *SAE Tech Paper*, No. 910675, February, 1991.

[25] J.J. White, J.N. Carroll, C.T. Hare and J.G. Lourenco, "Emission Control Stra-tegies for Small Utility Engines," *SAE Tech Paper*, No. 911807, SAE Intl Off-Highway & Powerplant Congress & Expo, Milwaukee, Wisconsin, September 9-12, 1991.

[26] P.H.Rochelle, "Delayed Charging: A Means to Improve Two-Stroke Engine Characteristics," *SAE Tech Paper*, No. 941678, SAE Intl Off-Highway & Power-plant Congress & Expo, Milwaukee, Wisconsin, September 12-14, 1994.

[27] R.B. Poola, B. Nagalingam, K.V. Gopalakrishnan, "Performance of Thin-Ceramic-Coated Combustion Chamber with Gasoline and Methanol as Fuels in a Two-Stroke SI Engine," *SAE Tech Paper*, No. 941911, SAE Intl Fuels & Lubricants Mtg & Expo, Baltimore, Maryland, October 17-20, 1994.

[28] K. Tsuchiya, Y. Nagai and T. Gotoh, "A Study of Irregular Combustion in Two-Stroke Cycle Gasoline Engines," *SAE Tech Paper*, No. 830091, SAE Intl Congress & Expo, Detroit,

Michigan, 1983.
[29] M. Abraham and S. Prakash, "A Theory of Cyclic Variations in Small Two-Stroke Cycle Spark Ignited Engines - An Analytical Validation of Experimentally Oserved Behaviour," *SAE Tech Paper*, No. 920426 , SAE Intl Congress & Expo, Detroit, Michigan, 1992.
[30] M. Abraham and S. Prakash, "Cyclic Variations in a Small Two-Stroke Cycle Spark-Ignited Engine - An Experimental Study," *SAE Tech Paper*, No. 920427, SAE Intl Congress & Expo, Detroit, Michigan, 1992.
[31] V. Sathe, P.S. Myers and O.A. Uyehara, "Parametric Studies Using a Two-Stroke Engine Cycle Simulation," *SAE Tech Paper*, No. 700124, SAE Auto Engrg Congress & Expo, Detroit, Michigan, 1970.
[32] G.P. Blair, "Prediction of Two-Cycle Engine Performance Characteristics," *SAE Tech Paper*, No. 760645, SAE Off-Highway Vehicle Mtg & Exhb, Milwaukee, Wisconsin, 1976.
[33] E. Sher, "The Effect of Atmospheric Conditions on the Performance of an Air-Borne Two-Stroke Spark-Ignition Engine," *I Mech E Proc*, Part D, Vol 198, No. 15, London, England, 1984.
[34] E. Sher, Y. Hacohen, S. Refael and R. Harari, "Minimizing Short-Circuiting Losses in 2-S Engines by Throttling the Exhaust Pipe," *SAE Tech Paper*, No. 901665, SAE Intl Off-Highway Congress & Expo, Milwaukee, Wisconsin, Sept. 10-13, 1990.
[35] R. Rohrer and B. Chehroudi, "Preliminary Heat Release Analysis in a Single-Cylinder Two-Stroke Production Engine," *SAE Tech Paper*, No. 930431, SAE Intl Congress &Expo, Detroit, Michigan, 1993.
[36] R. Harari and E. Sher, "The Effect of Ambient Pressure on the Performance Map of a Two-Stroke SI Engine," *SAE Tech Paper*, No. 930503, SAE Intl Congress & Expo, Detroit, Michigan, March 1-5, 1993.
[37] M.G. Reid and R. Douglas, "Quasi-Dimensional Modelling of Combustion in a Two-Stroke Cycle Spark Ignition Engine," *SAE Tech Paper*, No. 941680, SAE Intl Off-Highway & Powerplant Congress & Expo, Milwaukee, Wisconsin, September 12-14, 1994.
[38] M. Hallett (Editor), "High Praise," *Off-Road and 4 Wheel Drive*, Link House, U.K., March, 1990.
[39] D.Lock, "The End of the Additive ?," *Performance Ford*, vol 4, No. 2, pp 50-51, June, 1990.
[40] J.B.Heywood, *Internal Combustion Engine Fundamentals*, McGraw-Hill, New York,1988.
[41] C.R.Ferguson, *Internal Combustion Engines; Applied Thermosciences*," Wiley and Sons, New York, 1986.
[42] R.C. Reid, J.M. Prausnitz and T.K. Sherwood, *The Properties of Gases and Liquids*," 3rd Ed., McGraw-Hill, New York, 1977.
[43] G.J. Van Wylen and R.E. Sonntag, *Fundamentals of Classical Thermodynamics*, 3rd Ed., Wiley and Sons, New York, 1985.
[44] Y.A. Cengel and M.A. Boles, *Thermodynamics-An Engineering Approach*, McGraw- Hill, New York, 1989.
[45] J.H. Horlock and D.E. Winterbone (Editors), *The Thermodynamics and Gas Dynamics of Internal-Combustion Engines- Volume II*, pp. 782-785, Clarendon Press, Oxford, 1986.
[46] W.J.D. Annand and D. Pinfold, "Heat Transfer in the Cylinder of a Motored Reciprocating Engine," *SAE Tech Paper*, No. 800457, 1980.

APPENDIX (A)
Engine Specifications

Make and model	Sachs Stamo ST-151 2-Stroke, Single- cylinder crankcase-scavenged
Bore * stroke	60 mm * 54 mm
Compression ratio	8 : 1 (nominal)
Port timing	Suction opens 120° ATC closes 120° BTC Exhaust opens 95° ATC closes 95° BTC
Fuel system	Carburetor

Fuel and lubricant	Mixture of SAE 30 oil in premium gasoline (4:100).
Ignition system	Magneto
Ignition timing	22° 30' BTC ± 1° 50'
Maximum power	4.4 kW / 4500 RPM
Maximum torque	10.6 N.m / 3000 RPM

APPENDIX (B)
Scavenging-related Definitions

The delivery ratio DR is the ratio between the mass of the delivered mixture and the mass of the mixture that would fill the displaced volume at ambient pressure and temperature. This ratio corresponds to the volumetric efficiency in 4-stroke engines.

The trapping efficiency E_{tr} is the ratio between the mass of fresh mixture trapped in the cylinder at the beginning of effective compression and the mass of delivered mixture.

The scavenging efficiency E_{sc} is the ratio between the mass of fresh mixture trapped in the cylinder at the beginning of effective compression and the mass of all gases (fresh mixture + exhaust residue) trapped in the cylinder.

According to Heywood [40], the above ratios are interrelated by:

$$E_{tr} = E_{sc} \ / \ DR \qquad (B.1)$$

In real scavenging processes, mixing occurs as the fresh charge displaces the burned gases and some of the fresh charge may be expelled. Two extreme models of this process are:

- Perfect displacement (perfect scavenging) and
- Complete mixing.

Perfect displacement would occur if the burned gases were pushed out by the fresh gases without any mixing. On the other hand, complete mixing occurs uniformly with the cylinder contents.

For perfect displacement,

$$E_{sc} = DR \ , \ E_{tr} = 1 \quad \text{for} \quad DR \leq 1 \qquad (B.2.a)$$

$$E_{sc} = 1 \ , \ E_{tr} = 1/DR \quad \text{for} \quad DR > 1 \qquad (B.2.b)$$

For complete mixing,

$$E_{sc} = 1 - \exp(-DR) \qquad (B.3.a)$$

$$E_{tr} = [1 - \exp(-DR)]/DR \qquad (B.3.b)$$

Since the determination of the trapping and scavenging efficiencies is one of the most complicated tasks, models usually assume either perfect displacement or complete mixing. The assumption is reasonable because calibration studies [40] show that loop-scavenged and cross-scavenged engines can be modeled using the complete-mixing assumption, which is the case in the present investigation. On the other hand, uniflow-scavenged engines can be modeled according to the perfect-displacement assumption.

APPENDIX (C)
Models of Heat Release

Among the most common models of heat release are:

1. The linear model,

$$x = (\theta - \theta_1)/(\theta_2 - \theta_1) \qquad (C.1)$$

2. The sinusoidal model,

$$x = 0.5 - 0.5\cos[\pi(\theta - \theta_1)/(\theta_2 - \theta_1)] \qquad (C.2)$$

3. The exponential model,

$$x = 1 - 1/\exp[(\theta - \theta_1)/(\theta_2 - \theta_1)]^N \qquad (C.3)$$

where,

x is the mass fraction of fuel burned
θ_1 is the crank angle of onset of heat release
θ_2 is the crank angle of extinction of heat release
N is the exponential index of heat release.

In the above equations, the angle θ_1 is determined from the P-θ record as the angle at which a detectable rise of pressure takes place. The angle θ_2 is determined either by photographing combustion events (if possible) or from correlations available in the literature. The value of the index N depends on the experimental conditions, and is normally in the range of 4 to 7. More details are given in References [31], [32], [35], [40], and [41].